Single chain structure in thin polymer films: corrections to Flory's and Silberberg's hypotheses

2005 J. Phys.: Condens. Matter 17 S1697

(http://iopscience.iop.org/0953-8984/17/20/004)

INSTITUTE OF PHYSICS PUBLISHING JOURNAL OF PHYSICS: CONDENSED MATTER

J. Phys.: Condens. Matter **17** (2005) S1697–S1709 doi:10.1088/0953-8984/17/20/004

Single chain structure in thin polymer films: corrections to Flory's and Silberberg's hypotheses

A Cavallo[1], M Müller[2], J P Wittmer[3], A Johner[3] and K Binder[1]

[1] Institut für Physik, Johannes Gutenberg Universität, Staudinger Weg 7, D-55099 Mainz, Germany
[2] Department of Physics, University of Wisconsin-Madison, 1150 University Avenue, Madison, WI 53706-1390, USA
[3] Institut Charles Sadron, 6 Rue Boussingault, 67083 Strasbourg, France

Received 9 December 2004, in final form 1 January 2005
Published 6 May 2005
Online at stacks.iop.org/JPhysCM/17/S1697

Abstract

Conformational properties of polymer melts confined between two hard structureless walls are investigated by Monte Carlo simulation of the bond fluctuation model. Parallel and perpendicular components of chain extension, bond–bond correlation function and structure factor are computed and compared with recent theoretical approaches attempting to go beyond Flory's and Silberberg's hypotheses. We demonstrate that for ultrathin films where the thickness, H, is smaller than the excluded volume screening length (blob size), ξ, the chain size parallel to the walls diverges logarithmically, $R^2/2N \approx b^2 + c\log(N)$ with $c \sim 1/H$. The corresponding bond–bond correlation function decreases like a power law, $C(s) = d/s^{\omega}$ with s being the curvilinear distance between bonds and $\omega = 1$. Upon increasing the film thickness, H, we find—in contrast to Flory's hypothesis—the bulk exponent $\omega = 3/2$ and, more importantly, a *decreasing* $d(H)$ that gives direct evidence for an *enhanced* self-interaction of chain segments reflected at the walls. Systematic deviations from the Kratky plateau as a function of H are found for the single chain form factor parallel to the walls in agreement with the *non-monotonic* behaviour predicted by theory. This structure in the Kratky plateau might give rise to an erroneous estimation of the chain extension from scattering experiments. For large H the deviations are linear with the wavevector, q, but are very weak. In contrast, for ultrathin films, $H < \xi$, very strong corrections (albeit logarithmic in q) are found suggesting a possible experimental verification of our results.

(Some figures in this article are in colour only in the electronic version)

1. Introduction

The excluded volume interaction or self-repulsion of the segments along an isolated chain leads to self-avoiding walk statistics of long polymers in dilute solution [1–7]. The chain extension as

measured by the mean squared end-to-end distance, R^2, increases like a power law $R \sim N^{\nu_{SAW}}$ with chain length N. The exponent adopts the non-trivial value $\nu_{SAW} = 0.588\cdots$. The chains swell in order to reduce intramolecular interactions [1, 6].

In a semi-dilute solution or a melt, however, these excluded volume interactions are screened on length scales larger than the size of the 'blob', ξ [1–3, 6]. For distances smaller than ξ the chain statistics obeys self-avoiding statistics while for larger distances the chains adopt Gaussian conformations which are characterized by the exponent $\nu = 1/2$. On large distances the chains cannot reduce the segmental repulsion by increasing their spatial extension; the majority of excluded volume interactions stem from intermolecular contacts [1].

The concept of screening of excluded volume interactions in a dense polymer melt—the Flory hypothesis—plays a pivotal role in modern theory of polymer melts and concentrated solutions. It has been corroborated by Edwards [3, 8] and is borne out of renormalization group calculations [6]. The description of chain conformations as Gaussian random walks lies at the heart of many analytical or numerical approaches, for instance, the self-consistent field theory [9, 10] which has been widely used to describe spatially inhomogeneous polymer systems like surfaces of polymer melts, interfaces in polymer blends and self-assembly of copolymer systems.

One consequence of screening of excluded volume interactions on length scales larger than ξ is the behaviour in a thin film (see figure 1) [11]: if the chains were describable by random walks without *long ranged* interactions the properties parallel and perpendicular to the film surfaces would decouple. According to Silberberg's hypothesis [12] the chain conformations could be conceived as random walks reflected at the film surfaces, i.e., parallel chain extensions would remain unperturbed.

As we decrease the film thickness, H, the chain folds back into the volume occupied by their coil and other chains are expelled from that region. Silberberg's hypothesis has to break down if the self-density is comparable to the segmental number density of the bulk melt, ρ, i.e., $\rho R^2 H \sim N$ [13, 14]. For $H \ll \xi$ the chains adopt quasi-two-dimensional configurations [2] and the number of intermolecular contacts is strongly reduced. This is illustrated in figure 1(b).

While these phenomenological considerations yield a description of the leading *scaling behaviour* of large scale chain conformations, there are subtle corrections that may lead to significant deviations: renormalization group calculations provide great insight into the way excluded volume interactions are screened upon increasing the density and the crossing over from dilute to semi-dilute solutions [2, 4, 6]. These calculations predict the blob size, ξ, and the chain extension, R, as a function of the strength of the excluded volume interaction and the segmental density, ρ. They also provide information about the crossover from self-avoiding walk behaviour to Gaussian statistics upon increasing the distance along the chain in semi-dilute solutions. Surprisingly, renormalization group calculations by Schäfer [6] and Monte Carlo (MC) simulations [15, 13] of the bond fluctuation model revealed deviations from the plateau in the Kratky plot $q^2 S(q)$ versus q which were traced back to a Goldstone-type singularity. These deviations from the plateau in the Kratky plot indicated deviations from the Gaussian behaviour on length scales *larger* than ξ. Upon confining the chains into a thin film, one observes an increase of the deviations from the Gaussian behaviour [13, 14].

Recently, the statistics of quasi-two-dimensional polymer melts (called 'self-avoiding trails') has been studied by Semenov and Johner [11]. This model corresponds to polymers confined to ultrathin films, $H \ll \xi$, where, however, chains and chain segments are still allowed to overlap, as opposed to the pure two-dimensional limit ($H \to 0$) which has been considered thoroughly in the past resulting in beautiful analytical predictions [16] and more recent numerical tests [17–20]. Rather than calculating the chain extension as a function of density and strength of the excluded volume interaction, Semenov and Johner consider the

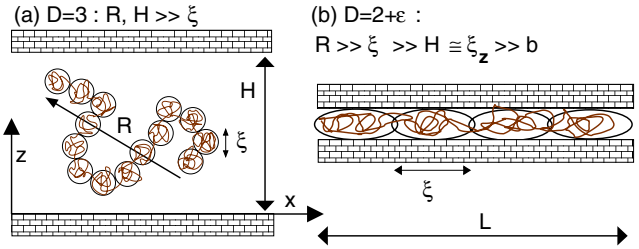

Figure 1. Schematic illustration of a polymer chain with typical size R confined between two parallel hard and structureless walls at a distance H. The z-axis is perpendicular to the lower wall. Periodic boundary conditions are used in x and y directions. (a) When $\xi \ll R \ll H$, ξ being the excluded volume blob size, coils far from the walls are unperturbed, i.e., $R_\alpha = R_{\text{bulk}}$ for all components $\alpha = x, y, z$. According to Flory and Edwards, they can be represented, to a first approximation, as Gaussian chains of blobs of size ξ. For chains (or chain sections) close to the walls it is generally assumed that they may be reflected at the walls but remain Gaussian. (b) For $H \simeq \xi \ll R_{\text{bulk}}$, the coils become effectively two-dimensional, but are still allowed to overlap and to cross in the two-dimensional projection. These are called $D = 2+\epsilon$ systems in contrast to a purely $D = 2$ films where intersections are forbidden and the coils become compact. It is illustrated that in the $D = 2+\epsilon$ case, the correlation length parallel to the film surfaces differs from H.

residual excluded volume interaction which is a weak perturbation to Gaussianity for $D = 3$; but is marginal, i.e., has to be renormalized, in ultrathin layers. This allows for quantitative predictions in the melt regime both for films and in the bulk. In contrast to Silberberg's argument, the chain extension for these $D = 2+\epsilon$ systems is predicted to exhibit logarithmic corrections,

$$R_\alpha^2(N)/2N = b(H)^2 + c(H)\log N, \tag{1}$$

for the parallel components ($\alpha = x, y$) of the end-to-end distance with respect to the walls. The first coefficient, b, corresponding to the statistical segment length is predicted to depend only very weakly on H [11]. The second coefficient $c(H)$ should be positive and inversely proportional to the number of particles per unit surface and, hence, inversely proportional to the film thickness, H. Likewise, one finds in the bulk ($D = 3$)

$$R_\alpha^2(N)/2N = b^2(\rho) - c(\rho)/\sqrt{N} \tag{2}$$

for any component $\alpha = x, y, z$ of the chain end-to-end vector [21]. Note that the second coefficient decreases now inversely with the monomer density. In both cases, the coefficient c of the leading correction term does not depend on the excluded volume parameter, v, expressing the fact that the corrections are due to the large scale incompressibility of the polymer melt [11, 21].

In our paper we numerically investigate the chain statistics in thin polymer films paying particular attention to residual excluded volume effects and their dependence on the film thickness. As sketched in figure 1, our computational study covers the regime from thick films, $H > R$, to ultrathin films, $H < \xi$, and allows us to investigate the crossover from the bulk behaviour ($D = 3$) over ultrathin films ($D = 2+\epsilon$) up to purely two-dimensional systems ($D = 2$). In the next section we describe the model and the simulation technique. Then we investigate the chain extensions parallel and perpendicular to the film, the bond–bond correlation function and the single chain structure factor. The final section presents our conclusion.

2. Computational model and some technicalities

Coarse-grained models are very efficient for investigating the universal properties of dense polymer systems. In such models, one integrates over the microscopic degrees of freedom, which do not affect the universal physical laws, but only their prefactors and local properties. In this work we have used the 'bond fluctuation model' (BFM)—a lattice Monte Carlo scheme where a monomer occupies eight lattice sites (i.e., the volume fraction $\phi = 8\rho$, ρ being the number density) and the bonds, $\mathbf{l}$, between adjacent monomers can vary in length and direction, subject only to excluded volume constraints and entanglement restrictions [22, 24]. The BFM has been extensively studied in the past [9, 15, 13, 17, 18, 21, 23, 25].

Chain configurations are updated by two kinds of canonical moves: random monomer hoppings and slithering snake (or reptation) moves [24]. In the first case we consider random displacements of an effective monomer by one lattice site in one of the six possible directions in the lattice. These moves are efficient in relaxing the local properties of the chain, such as the bond angle or the bond length. In slithering snake moves, a segment of the chain is removed from one end and added to the opposite end of the chain in a random direction. The latter moves relax the chain conformation a factor N faster than the random monomer hoppings. (See [25] for details on the exponential increase of the relaxation time for very long chains due to correlations in the slithering snake motion.)

As illustrated in figure 1, we use an $L \times L \times H$ box with hard walls at $z = 0$ and $H + 1$, i.e., the thinnest film with $H = 2$ corresponds to a pure $D = 2$ system where chains are not allowed to overlap. For $H = 4$ this becomes possible and, therefore, this is an ideal system for testing the predictions of [11]. We have systematically varied the film thickness from $H = 2$ up to $H = 84$ while keeping the dimensions parallel to the walls fixed at $L = 256$ (with the exception that $L(H = 2) = 512$). Periodic boundary conditions have been used in x and y directions. Note that L is always much larger than R_x, the typical chain size component parallel to the walls.

The chain length ranged from $N = 16$ up to 256. We have concentrated in this study on dense polymer melts and all the data reported here are for a number density $\rho = 0.5/8$. For this density the (bulk) excluded volume blob size is $\xi \approx 7$ [23].

We used the configurational bias method to create the initial configurations for chain lengths up to $N = 64$. (The longest chain length possible numerically with this method decreases with H.) To this end a chain is grown monomer by monomer into the system taking into account all possible bond vectors for the next monomer. From those positions of the next monomer, one that does not overlap with any other monomer in the system is chosen at random. This choice introduces a bias which is removed by the Metropolis acceptance criterion once the chain is fully grown. For larger N, we started with relatively compact two-dimensional coils ($R \sim N^{1/2}$) oriented parallel to the surfaces. In all cases we equilibrate our systems using a mixture of local and slithering snake moves which has been found to be the most efficient [25]. Some of our configurations have already been used in some recent related investigations on thin polymer films [14, 18].

Various static and dynamical properties parallel and perpendicular to the walls have been measured on the fly and for a more detailed analysis configurations were periodically stored. Since the x and y directions parallel to the walls are equivalent these properties are averaged together. If not specified otherwise, properties are averaged over all chains irrespective of their distance to the walls. For later reference, we note here the bulk values for the end-to-end distance $R \approx 49.8$ and the radius of gyration $R_g \approx 20.3$ for chains of length $N = 256$. The three components of the mean squared bond vector $l_\alpha \equiv \langle l_\alpha^2 \rangle^{1/2} \approx 1.52$ of the bulk remain unchanged for all $H > 7$. Obviously, the perpendicular component must ultimately vanish

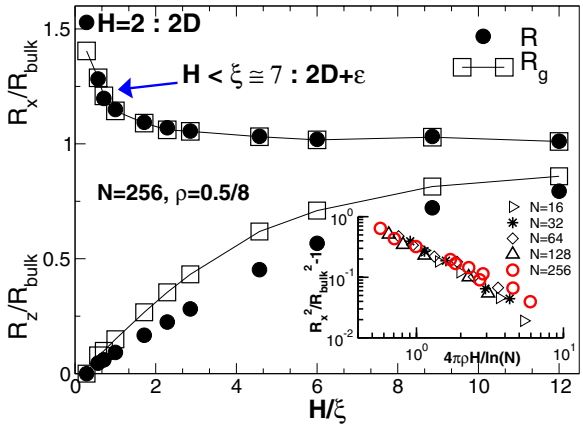

Figure 2. Parallel and perpendicular components of end-to-end distance R (closed symbols) and of radius of gyration R_g (open symbols) for $N = 256$ as a function of the film thickness H. All the quantities are normalized with respect to the corresponding bulk value. The data are averaged over all chains in the film irrespective of the distance of their centre of mass from the walls. The (reduced) parallel components remain constant for distances larger than the characteristic width $H^\star$ which for the chain length used is of the order of ξ. The bulk value of ξ for the volume fraction presented is indicated. Note that for $H = 2$ no chain overlap is possible in our model and the chains are rigorously two-dimensional. $D = 2 + \epsilon$ behaviour is expected for $2 < H < \xi$. The perpendicular component increases continuously with H. The effect is linear for $H \ll R_{\rm bulk}$, as one expects. The inset presents the chain length dependence of the parallel chain dimensions as a function of $H/H^\star$ for different chain lengths, N, as indicated in the key. The nice scaling collapse found confirms the predicted logarithmic dependence of $H^\star$ and is one central finding of this work.

and the parallel component increase. For $H = 4$ we find, for example, $l_x = l_y = 1.63$ and $l_z = 1.2$.

3. Results

We discuss now in turn three intra-chain properties: the global chain size $R_\alpha(N, H)$, the bond–bond correlation function $C_\alpha(s)$ as a function of curvilinear distance s along the molecule's backbone and the form factor $S_\alpha(q)$.

3.1. End-to-end distance and radius of gyration

We start the discussion by presenting the chain size as measured by the three components $R_\alpha^2 \equiv \langle (r_{\alpha,N} - r_{\alpha,1})^2 \rangle$ of the end-to-end distance R and the corresponding components of the radius of gyration R_g. Here, $r_{\alpha,n}$ denotes the α-component of the position of the nth monomer of the chain.

In figure 2 we present the end-to-end distance and the radius of gyration, R_g, as a function of the film thickness H. The data are normalized by the corresponding bulk value, i.e., all the ratios must become unity for large H. Only data for chain length $N = 256$ have been included. As expected, the thinner the film, the larger the component parallel to the surface and the smaller the perpendicular one. The perpendicular component increases continuously with H. The effect is linear for $H \ll R_{\rm bulk}$, as one expects even for perfectly Gaussian chains. Note that the perpendicular component of R_g increases more rapidly as the component of the end-to-end vector for small H. In agreement with [11] the (reduced) parallel components remain

constant for $H \gg H^\star \approx \xi \approx 7$, but increase rapidly for thinner films. (We recall that for $H = 2$ no chain overlap is possible in our model and the chains are rigorously two-dimensional.) This demonstrates that perpendicular and parallel components of the polymer couple, in contrast to Silberberg's hypothesis. Note that the observed chain length dependence of the crossover slit width $H^\star$ is relatively weak for the chain lengths we have probed (cf figure 2 inset). This is in line with the predicted *logarithmic* increase $H^\star \approx \xi \log(N/g)$, $g \sim \xi^2$ denoting the number of monomers contained in the excluded volume blob, which follows readily from the condition $\rho R^2 H^\star \sim N$ utilizing equations (1) and (2) [11].

In the next figure we present the parallel component of the end-to-end vector, R_x, as a function of N for different H. Also included are the data for bulk systems ($D = 3$) without walls and periodic boundary conditions in all directions. In agreement with equation (2) we find corrections to ideality even in this latter case. For details the reader is referred to the recent study [21]. As expected, the reduced data for both $D = 3$ and 2 limits ($H = 2$) become chain length independent for long enough chains. (Note that the chain size for $D = 2$ is $R_x \sim N^{1/2}$ without logarithmic correction [16].) More interestingly, we find that all intermediate data *diverge logarithmically* for long enough chains (thin lines). Extrapolating our data, one even expects that for $N \gg 2000$ and $H = 4$ the chains will become actually larger than the pure $D = 2$ ones. In their work Semenov and Johner [11] have predicted for the slope in log-linear coordinates (cf equation (1))

$$1/c = 4\pi c_0 = 4\pi\rho H \tag{3}$$

where c_0 is the number of particles per unit surface. Hence, the coefficient decreases inversely with H. In contrast, the first coefficient, b, of equation (1) is predicted to depend only very weakly on H [11]. Using equation (3) and adjusting $b(H)$ we obtain rather good agreement with the numerical data. This is the central result of this work. Note that $b(H)$ is essentially constant as can be seen from the convergence of the lines for small N. We even get acceptable fits for film widths three times larger than ξ, which is consistent with the logarithmic increase of $H^\star$ with chain length mentioned above.

We have also investigated the components of the mean squared distance along the chain $R_\alpha^2(s) \equiv \langle (r_{\alpha,n} - r_{\alpha,n+s})^2 \rangle_n$ obtained by averaging over all chains and all pairs of monomers separated by a curvilinear distance $s = |m - n|$ along a chain. Here, $\langle \cdots \rangle_n$ denotes the average over all couples of bonds having curvilinear distance s and over all polymers in the system. The predictions of [11, 21], equations (1) and (2), generalize readily from $s = N$ to arbitrary curvilinear distance. This is well confirmed by our data which look quite similar to those given in figure 3. Instead of discussing these data we will rather proceed by discussing the numerically more challenging *curvature* of $R_\alpha(s)$, i.e., by presenting our results on the bond–bond correlation function, which allows a much more accurate test of the predictions.

3.2. Bond–bond correlation function

The connection between the mean squared distance between two segments n and m along the chain and the bond–bond correlation function is due to the exact formula

$$\langle l_{\alpha,n} l_{\alpha,m} \rangle = -\frac{1}{2} \frac{\partial^2}{\partial m \partial n} \langle (r_{\alpha,n} - r_{\alpha,m})^2 \rangle \tag{4}$$

valid for $\alpha = x, y, z$. Note that the bond vector is defined as $\mathbf{l}_n = \mathbf{r}_{n+1} - \mathbf{r}_n \approx \partial \mathbf{r}_n / \partial n$, the latter identity becoming true in the continuous limit. More generally, equation (4) may be written in terms of the difference operator $\Delta_n f(n) = f(n+1) - f(n)$. In that sense, it remains valid for arbitrary curves, $\mathbf{r}_n$, even for non-differentiable Brownian walks.

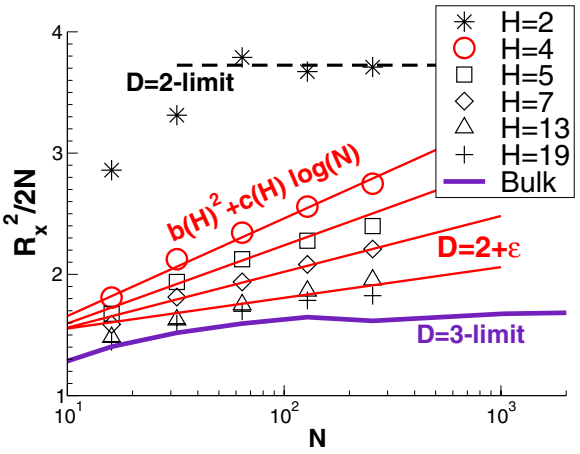

Figure 3. Parallel components of the end-to-end distance for different H as a function of chain length N. We plot $R_x^2/2N$ in log-linear coordinates to demonstrate the expected logarithmic divergence for $D = 2 + \epsilon$ systems [11]. The thin lines compare with the prediction, equations (1), (3), where we directly verify $c(H) = 1/4\pi\rho H$ and fit for the coefficient $b(H)$ which is found to depend very weakly on the film width becoming ultimately H independent (left side of figure). The pure $D = 2$ data ($H = 2$, stars) become chain length independent for chain lengths $N \geqslant 64$ (dashed line). Note that even the bulk data are monotonically increasing in agreement with equation (2).

Averaging again over all pairs $(n, m = n+s)$ we have computed the correlation functions $C_\alpha(s) = \langle l_{\alpha,n} l_{\alpha,n+s}\rangle_n / l_\alpha^2$.[4] Neglecting chain end effects and using equation (4) one obtains the compact relation $2C_\alpha(s)l_\alpha^2 = \partial_s^2 R_\alpha^2(s)$ between the two curvilinear properties.

From equations (1) and (2), generalized to arbitrary s, we immediately see that the bond–bond correlation function must become

$$C_\alpha(s) = ds^{-\omega} \tag{5}$$

with a prefactor $d \sim 1/\rho$ and an exponent $\omega = 3/2$ for the bulk and $d = c/l_\alpha^2$, $\omega = 1$ for ultrathin films. Noticeably, the long distance behaviour of $C_\alpha(s)$ is not characterized by a length scale (persistence length) but the residual excluded volume interaction change the dominant scaling behaviour to a scale-free power law. This is in marked contrast to the Flory hypothesis where long ranged correlations between bonds are neglected and $C_\alpha(s)$ is assumed to decay exponentially (or even faster) [21]. The technical advantage of the bond–bond correlation function compared with the curvilinear distance is that it does not depend on the trivial, but very large Gaussian contribution which drops out after differentiating. Hence, it allows us to focus directly on the corrections to the Gaussian behaviour on large length scales.

In figure 4 the perpendicular bond–bond correlation function, $C_z(s)$, is plotted as a function of the curvilinear distance, s, for chain length $N = 256$ and different film thicknesses, H. For very thin films negative correlations at short distances can be observed. For $H = 4$ and 5, on average, the angle ϑ between two consecutive bonds, in the direction perpendicular to the walls, is larger than 90° (i.e., the two vectors have opposite direction). For $H = 7$, the correlations reach the minimum for $s = 2$. This means that chains fold back every two monomers. These results are a trivial consequence of confinement. For very thin films, due to strong fluctuations of the density as a function of the distance from the walls, the system essentially consists of

[4] We have compared this definition to $\langle e_{\alpha,n} e_{\alpha,n+s}\rangle_n$ for the normalized bond vector $\mathbf{e}_n$ without finding any measurable difference. This might be due to the weak correlation between bond length and bond angle fluctuations.

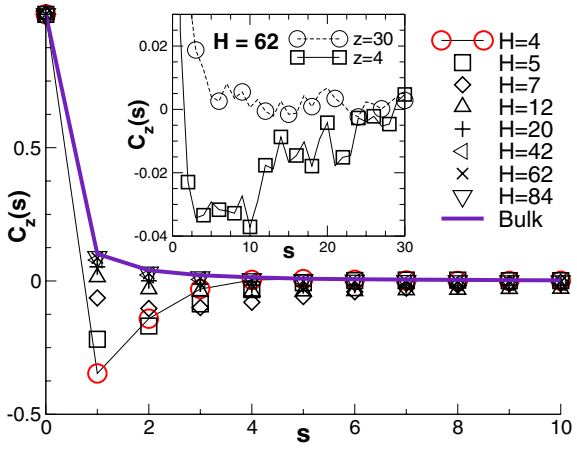

Figure 4. Perpendicular bond–bond correlation function, $C_z(s)$, versus curvilinear distance, s, between monomers for $N = 256$ and different film thicknesses, H. The inset shows the behaviour of the same correlation function for polymers with centres of mass at distances $z = 4$ and 30 from the wall at $z = 0$ in a film with $H = 62$.

the superposition of monolayers with distance equal to the lattice spacing. For $H = 4$ and 5 we have two layers; then two consecutive segments along the chain are prevalently located in different planes and the chain is reflected at the surface. For $H = 7$, we have one more layer and then up to three linked monomers can be placed at different heights. Upon increasing the film thickness, H, above the blob size, ξ, $C_z(s)$ gradually tends to the curve obtained in the bulk.

The same effect can also be observed for thicker films taking into account only chains with the centre of mass having a distance, z, from the walls smaller than ξ. This is a consequence of excluded volume effects in the direction perpendicular to the wall which give rise to a strong anisotropic deformation of the coil. In the inset of figure 4 we show $C_z(s)$ calculated for polymers with different distances, z, of their centres of mass from the surface. In this plot we compare the curves obtained for $z = 4$ and 30 in a film with $H = 62$. While in the first case the interactions with the wall must be very strong the walls should have a negligible effect on the latter where the chains are exactly located in the middle of the film. Indeed, only in the first case can evident negative correlations be seen and we recover bulk behaviour in the second. The insufficient statistics prevents a precise location of the minimum for $z = 4$. This value roughly corresponds to $s = 5$ which is close to the distance of the centre of mass from the wall.

A quantitative analysis of the decay of $C_x(s)$ is given in figure 5 where we plot the function on a double logarithmic scale. The curves can be fitted rather well by power laws, in agreement with equation (5), and exponential behaviour can definitely be ruled out for long enough chains. Obviously, this is a clear-cut contradiction to Flory's and Silberberg's descriptions. For large thicknesses, $H > 7 \approx \xi$, we observe the expected bulk exponent $\omega = 3/2$. Interestingly, the prefactor, d, increases as we decrease the film thickness, H, although the exponent remains constant. This shift can be related to the dependence on the fraction of polymers $\propto 1/H$ which interact with the surface. Chain segments close to the wall have increased bond–bond correlations $\langle l_{x,n} l_{x,n+s} \rangle$ due to the enhanced self-interaction of the segment which is, in turn, due to the reflection of the segment at the wall. To first order, the reflections may still be described by Gaussian statistics. As H increases and the relative population of chain segments of size s

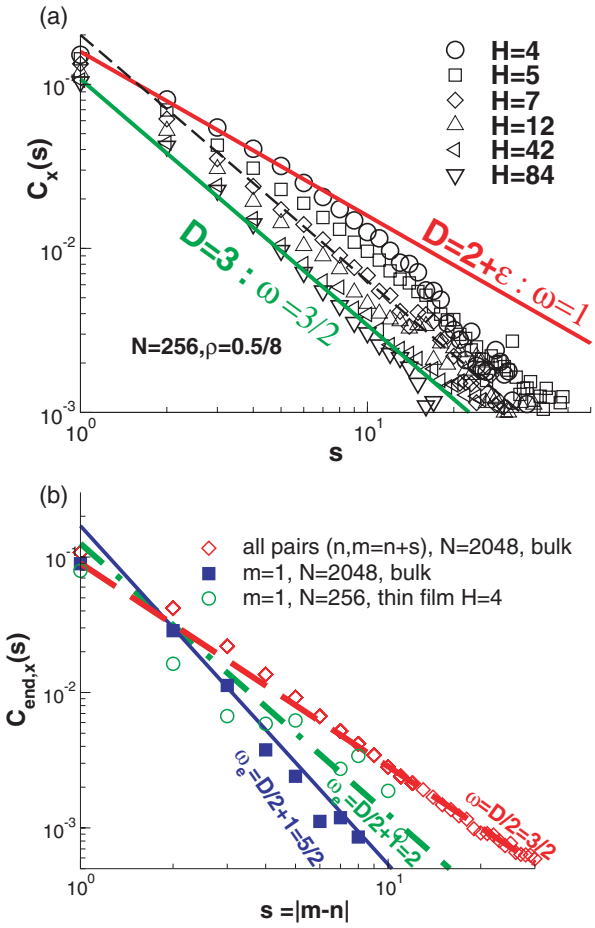

Figure 5. (a) Log–log plot of $C_x(s)$ versus s for different film thicknesses and for $N = 256$. The lines indicate the power law behaviour, $C_x(s) = d(H)/s^{\omega}$, predicted for different regimes. The slope $\omega = 3/2$ (bottom line) is expected for bulk systems and larger slits. While this exponent remains unchanged for $H \gg \xi$ the amplitude $d(H)$ does not. As indicated by the broken line, we demonstrate a systematic *increase* with decreasing H. Finally, for $D = 2+\epsilon$ films our data confirm the exponent $\omega = 1$ (upper bold line) implicit in the work of Semenov and Johner [11]. (b) Double logarithmic plot of $C_{\mathrm{end},x}(s)$ in the bulk and a thin film, $H = 4$, corresponding to $D = 2+\epsilon$. The bulk correlation function averaged over all pairs is shown as a reference. The predicted power laws are indicated by straight lines.

decreases the amplitude must decrease. This interpretation has been directly confirmed by computing, as in figure 4, $C_x(s)$ for various distances, z, of the chain centre of mass from the walls (not shown). For ultrathin $D = 2+\epsilon$ films, the bulk exponent must break down. Indeed, our data are still compatible with a power law but with the exponent $\omega = 1$ predicted for this regime.

Since finite-chain size effects could be crucial here, larger chains are needed to rigorously establish the exponent over more than a decade in s. In the bulk the correlation function decays more rapidly for short chains and its explicit dependence on N has been obtained [21]. This is, in part, due to the behaviour close to the chain ends. In the analysis we have averaged the correlations over all pairs with the same distance, s, along the chain's contour but neglected

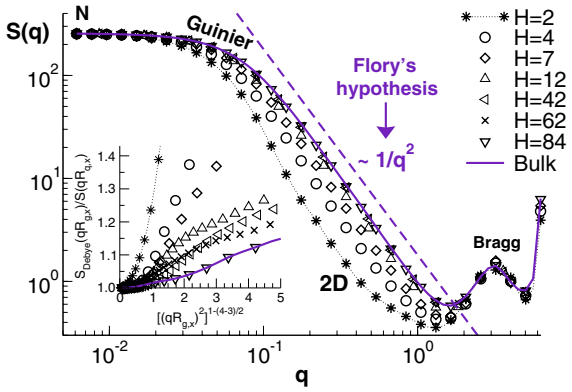

Figure 6. Single chain form factor for wavevectors q parallel to the wall surfaces for different H. Only data for $N = 256$ and $\rho = 0.5/8$ are considered. The bulk result ($H \to \infty$) is given by the bold line; Flory's hypothesis is indicated by the broken line. The Bragg limit ($q > 1$) is not affected by the presence of the walls. However, this can be clearly seen for larger length scales where the scattering amplitude goes systematically down with decreasing film width. The effect is the most prominent for the $D = 2$ system (stars), but even there the Bragg peak is not altered. The inset presents the ratio of the structure factor, S_{Debye}, of a Gaussian chain with the measured radius of gyration and the structure factor, $S(q)$, observed in the simulations as a function of $\sqrt{(qR_{gx})^2}$.

chain end effects. This is permissible for large N.[5] Interestingly, the correlation function measured from a chain end, $C_{\text{end},\alpha}(s) \equiv \langle l_{\alpha,0} l_{\alpha,s} \rangle_n / l_\alpha^2$, decays with a different, stronger exponent, $\omega_e = D/2 + 1$. The simulation results are presented in panel (b) of figure 5. For bulk melts, very long chains are available [21] and confirm the value of the exponent, $\omega_e = 5/2$ for $D = 3$. The data for thin films are also compatible with the theoretical prediction.

3.3. Form factor $S(q)$

The single chain form factor

$$S(q) = \frac{1}{N} \sum_{n,m=1}^{N} \left\langle \exp\left(\mathrm{i} \sum_\alpha q_\alpha (r_{\alpha,n} - r_{\alpha,m}) \right) \right\rangle \tag{6}$$

of a chain is an important, experimentally relevant quantity. The components of the scattered radiation vector are denoted by q_α. We are only interested here in the internal correlations parallel to the wall and, hence, consider only wavevectors parallel to the surface ($q_z = 0$) and omit the index in the following.

In figure 6 we present $S(q)$ for different film thicknesses and chain length $N = 256$. The analogous quantity, calculated for the bulk system, is also depicted as a reference curve. For small q the form factor just counts the number of scattering units; for large q it probes the structure on the scale of the monomers, the so-called Bragg peak. Not surprisingly, in both limits $S(q)$ does not depend on the presence of walls. For small q the data should be described by the rather general expansion $S(q) = N[1 - (R_{gx} q)^2 + \cdots]$ due to Guinier [3]. Here, $R_{gx}(H)$ stands for the measured parallel component of the radius of gyration. Since R_{gx} increases for small H (figure 2) the structure factor should decrease in agreement with what can be seen in the figure. One can check explicitly for all H that Guinier's formula applies. Hence, the

[5] The dependence of correlations on the position along the chain has recently been studied for isolated, self-repelling polymer chains by Schäfer and Elsner [26].

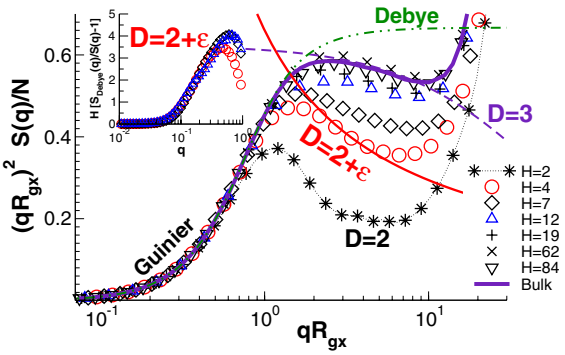

Figure 7. Kratky plot $(qR_{gx})^2 S(q)/N$ versus qR_{gx} for wavevectors parallel to the walls using the same symbols as in the previous plot. We have rescaled the data with the chain length N and R_{gx}, the measured component of the radius of gyration parallel to the surface. We see that the density fluctuations get systematically suppressed with decreasing film width H. The data for $H = 4$ have been compared with the logarithmic correction, equation (7), proposed in [11] and the bulk data (bold line) with the corresponding linear relationship (dashed line). The dashed–dotted line indicates the Debye functions $S_{\mathrm{Debye}}(qR_{gx})/N$. The inset presents the deviation, $S_{\mathrm{Debye}}(q)/S(q) - 1$, of the measured form factor in thin films with $4 \leqslant H \leqslant 12$ from the Debye function for the same radius of gyration. As expected, for $1 > q > 1/R_{\mathrm{g}}$ the deviations grow logarithmically in q and the amplitude is proportional to $1/H$ as can be seen from the scaling collapse. The deviation decreases again for large q due to additional (non-universal) corrections in the Bragg limit which are not taken into account by the theory.

deviation from the bulk limit seen in this regime is fully described in terms of the increased chain size.

The Gaussian self-similar structure for intermediate length scales is the essence of Flory's hypothesis and results in a power law behaviour of the form $S(q) \sim 1/q^2$, which is indicated by the broken line. Broadly, this is confirmed by the thick films ($H \geqslant \xi$). Differences become more apparent when we plot the ratio of the structure factor of a Gaussian chain, S_{Debye}, with the same radius of gyration and the measured single chain structure factor. This ratio is presented in the inset of figure 6. The clearly observable deviations are already present in the bulk [15] and increase upon reducing the film thickness [13]. Significant differences with respect to Gaussianity are observed for the thin films.

The deviations from the Gaussian behaviour as well as the effect of the confinement are magnified in the Kratky plot shown in figure 7 where we have plotted $(qR_{gx})^2 S(q)/N$ versus qR_{gx} for $N = 256$. This plot illustrates a popular method for extracting the chain dimensions from scattering data. Using the measured value of the radius of gyration we obtain perfect scaling for the Guinier regime, $qR_{gx} < 1$. Not surprisingly, the scaling fails for very large q (Bragg peak) where the data diverge. More interestingly, the scaling fails even for intermediate wavevectors where it should hold for Gaussian statistics [15]. Instead we find a pronounced *non-monotonic* behaviour in stark contrast to traditional hypotheses. As already seen in the previous figure, the deviations get more pronounced with increased confinement [13]. Similar deviations are also observed in semi-dilute bulk solutions of long chains, $N = 2048$ [15].

These effects have been analytically predicted for semi-dilute solutions [15] and melts [11]. For $qR_{gx} \gg 1$ and for long chains[6]

$$\frac{S_{\mathrm{Debye}}(q)}{S(q)} - 1 = e(H) \log(qf(H)) \tag{7}$$

[6] For exponentially long chains yet another regime is expected [11] which is outside the reach of simulation.

has been suggested for thin films. Only the first of the two coefficients $e(H)$ and $f(H)$ should depend sufficiently strongly on the slit width to be measurable: $e(H) \sim c(H) \sim 1/H$ [11]. $S_{\mathrm{Debye}}(q)$ denotes the structure factor of a Gaussian chain with identical radius of gyration. In the inset of figure 7 we explicitly verify the film thickness and wavevector dependence for $4 \leqslant H \leqslant 12$. It also confirms that $e(H)\log(f(H))$ is rather small. For $D = 3$ melts the deviation from the Kratky plot has been estimated more recently by Beckrich [27] using the perturbation approach of [11]. This yields the linear expression $\frac{S_{\mathrm{Debye}}(q)}{S(q)} - 1 = e(\rho)q$ which we have fitted to our bulk data (dashed line). A similar expression was derived for the limit of semi-dilute solutions ($\rho \ll 1$ but $\rho R^3/N \gg 1$) by Schäfer $S_{\mathrm{Debye}}(q)/S(q) - 1 = e'[(q\xi)^2]^{1-\epsilon/2} + \cdots$ where e' is a constant and $\epsilon = 4 - D$ [6]. Thus we expect corrections to the Kratky plot to be present over the entire concentration regime where the chains overlap. Since not all prefactors are explicitly available as a function of the model parameters of the BFM the test is less rigorous than the one in figure 3. While our simulation data are compatible with the theoretical predictions, longer chain lengths would clearly be desirable.

4. Conclusions

Using Monte Carlo simulations of long polymers confined between hard structureless walls we investigate deviations from the classical hypotheses of Flory [1] and Silberberg [12]. In agreement with recent theoretical work [11] on ultrathin films with $H < \xi$ we find that parallel and perpendicular components couple and the chain size parallel to the surfaces increases strongly. We quantitatively demonstrate the logarithmic divergence, equation (1), for the chain size parallel to the walls as a function of chain length, N. The prefactor $c \sim 1/H$ predicted for the logarithmic deviation allowed a rather accurate fit of our data. As emphasized in [11, 21], these effects are due to the chain connectivity and the large scale osmotic incompressibility of the solution and express universal physics independent of local properties.

Perhaps the most striking effect of this study is the power law asymptote for the bond–bond correlation function which measures the curvatures of the curvilinear distance along the chains. It allows a direct numerical test of the non-Gaussian corrections both in the bulk and in the ultrathin films and demonstrates the presence of long ranged correlations neglected by the classical hypotheses. Note that the decay exponent for both bulk and thin film geometry can be expressed in the form $\omega = \nu D$, D being the effective dimensionality of the system and $\nu = 1/2$ the characteristic exponent of a random walk. Interestingly, this is similar to the result obtained for the velocity correlation function of dense liquids in two and three dimensions [28].

An important consequence of our work arises for an experimentally relevant quantity, the static structure factor $S(q)$. In fact, simulation and theory show distinct non-monotonic behaviour of $q^2S(q)$ versus q (Kratky plot) due to the non-Gaussian corrections which even get enhanced with decreasing film width. This suggests a possible route for experimental verification and is a cause for serious concern as regards the standard operational definition and measure of the persistence length from the 'assumed' Kratky plateau.

Finally, we point out that the physical mechanism which has been sketched above is rather general and should not be altered by details such as a finite persistence length—at least not as long as the nematic ordering remains negligible. This is in fact confirmed by preliminary and on-going simulations.

Acknowledgments

We thank J Baschnagel, P Beckrich, S Obukhov and A N Semenov for useful discussions. AC thanks the MPI Mainz for a fellowship. Additional financial support from LEA, MOLSIMU,

ESF SUPERNET programmes is acknowledged as well as computational resources from the HLR Stuttgart, the NIC Jülich and IDRIS, Orsay.

References

[1] Flory P J 1988 *Statistical Mechanics of Chain Molecules* (New York: Oxford University Press)
[2] De Gennes P-G 1979 *Scaling Concepts in Polymer Physics* (Ithaca, NY: Cornell University Press)
[3] Doi M and Edwards S F 1986 *The Theory of Polymer Dynamics* (Oxford: Clarendon)
[4] des Cloizeaux J and Jannink G 1990 *Polymers in Solution* (Oxford: Clarendon)
[5] Grosberg A Y and Khokhlov A R 1994 *Statistical Physics of Macromolecules* (*AIP Series in Polymers and Complex Materials*) (New York: AIP)
[6] Schäfer L 1999 *Excluded Volume Effects in Polymer Solutions* (Heidelberg: Springer)
[7] Rubinstein M and Colby R H 2003 *Polymer Physics* (Oxford: Oxford University Press)
[8] Muthukumar M and Edwards S F 1982 *J. Chem. Phys.* **76** 2720
[9] Müller M 1998 *Macromolecules* **31** 9044
[10] Müller M 2005 Monte Carlo simulations and self-consistent field theory for thin polymer films *Handbook of Computational Nanotechnology* vol 10, ed R Rieth and W Schommers, American Scientific Publishers, pp 1–52
[11] Semenov A N and Johner A 2003 *Eur. Phys. J.* E **12** 469
[12] Silberberg A J 1982 *Colloid Interface Sci.* **90** 86
[13] Müller M 2002 *J. Chem. Phys.* **116** 9930
[14] Cavallo A, Müller M and Binder K 2005 *J. Phys. Chem.* B at press
[15] Müller M, Binder K and Schäfer L 2000 *Macromolecules* **33** 3902
[16] Eisenriegler E, Kremer K and Binder K 1982 *J. Chem. Phys.* **77** 6296
Duplantier B and Saleur H 1986 *Phys. Rev. Lett.* **57** 3179
Duplantier B and Saleur H 1987 *Phys. Rev. Lett.* **59** 539
[17] Carmesin I and Kremer K 1990 *J. Physique* **51** 915
[18] Cavallo A, Müller M and Binder K 2003 *Europhys. Lett.* **61** 214
[19] Yethiraj A 2003 *Macromolecules* **36** 5854
[20] Hehmeyer O J, Arya G and Panagiotopoulos A Z 2004 *J. Phys. Chem.* **108** 6809
[21] Wittmer J P *et al* 2004 *Phys. Rev. Lett.* **93** 147801
[22] Carmesin I and Kremer K 1988 *Macromolecules* **21** 2819
Deutsch H P and Binder K 1991 *J. Chem. Phys.* **94** 2294
[23] Paul W, Binder K, Heermann D and Kremer K 1991 *J. Physique* II **1** 37
[24] Baschnagel J, Wittmer J P and Meyer H 2004 Monte Carlo simulation of polymers: coarse-grained models *Computational Soft Matter: From Synthetic Polymers to Proteins* (*NIC Series* vol 23) ed N Attig *et al* pp 83–140 (*Preprint* cond-mat/0407717)
[25] Mattioni L *et al* 2003 *Eur. Phys. J.* E **10** 369
[26] Schäfer L and Elsner K 2004 *Eur. Phys. J.* E **13** 225
[27] Beckrich P 2004 private communication
[28] Alder B J and Wainwright T E 1970 *Phys. Rev.* A **1** 18
Hansen J P and McDonald I R 1986 *Theory of Simple Liquids* (New York: Academic)